JOURNAL OF MAGNETIC RESONANCE **135,** 104–112 (1998)
ARTICLE NO. MN981575

Computer Simulation of Magnetic Resonance Spectra Employing Homotopy

K. E. Gates,*,[1] M. Griffin,* G. R. Hanson,† and K. Burrage*

*Department of Mathematics and †Centre for Magnetic Resonance, The University of Queensland, St. Lucia, Queensland, 4072, Australia

E-mail: keg@maths.eq.edu.au

Received June 25, 1997; revised July 6, 1998

Multidimensional homotopy provides an efficient method for accurately tracing energy levels and hence transitions in the presence of energy level anticrossings and looping transitions. Herein we describe the application and implementation of homotopy to the analysis of continuous wave electron paramagnetic resonance spectra. The method can also be applied to electron nuclear double resonance, electron spin echo envelope modulation, solid-state nuclear magnetic resonance, and nuclear quadrupole resonance spectra. © 1998 Academic Press

Key Words: **electron paramagnetic resonance; computer simulation; homotopy; electron spin resonance.**

INTRODUCTION

Multifrequency electron paramagnetic resonance (EPR) spectroscopy (*1–3*) is a powerful tool for characterizing paramagnetic molecules or centres within molecules that contain one or more unpaired electrons. EPR spectra are often complex and are interpreted with the aid of a spin Hamiltonian. For an isolated paramagnetic centre (A) a general spin Hamiltonian is (*1–3*)

$$\mathcal{H}_A = \mathbf{S}\cdot D\cdot\mathbf{S} + \beta\mathbf{B}\cdot g\cdot\mathbf{S} + \mathbf{S}\cdot A\cdot\mathbf{I} + \mathbf{I}\cdot Q\cdot\mathbf{I} - \gamma\mathbf{I}\cdot(1-\sigma)\cdot\mathbf{B}, \quad [1]$$

where $\mathbf{S}$ and $\mathbf{I}$ are the electron and nuclear spin operators respectively, D the zero field splitting tensor, g and A are the electron Zeeman and hyperfine coupling matrices, respectively, Q is the quadrupole tensor, γ the nuclear gyromagnetic ratio, σ the chemical shift tensor, β the Bohr magneton, and $\mathbf{B}$ the applied magnetic field.

Additional hyperfine, quadrupole, and nuclear Zeeman interactions will be required when superhyperfine splitting is resolved in the experimental EPR spectrum. When two or more paramagnetic centres (A_i, $i = 1, \ldots, N$) interact, the EPR spectrum is described by a total spin Hamiltonian ($\mathcal{H}_{Total}$) which is the sum of the individual spin Hamiltonians ($\mathcal{H}_{A_i}$, Eq. [1]) for the isolated centres (A_i) and the interaction Hamiltonian ($\mathcal{H}_{A_{ij}}$) which accounts for the isotropic exchange, antisymmetric exchange, and the anisotropic spin–spin (dipole–dipole coupling) interactions between a pair of paramagnetic centres (*2–5*),

$$\mathcal{H}_{Total} = \sum_{i=1}^{N}\mathcal{H}_{A_i} + \sum_{i,j=1,j\neq i}^{N}\mathcal{H}_{A_{ij}}$$

$$\mathcal{H}_{A_{ij}} = J_{A_{ij}}\mathbf{S}_{\mathbf{A_i}}\cdot\mathbf{S}_{\mathbf{A_j}} + d_{A_{ij}}\mathbf{S}_{\mathbf{A_i}}\times\mathbf{S}_{\mathbf{A_j}} + \mathbf{S}_{\mathbf{A_i}}\cdot D_{A_{ij}}\cdot\mathbf{S}_{\mathbf{A_j}}. \quad [2]$$

Computer simulation of the experimental randomly orientated or single crystal EPR spectra from isolated or coupled paramagnetic centres is often the only means available for accurately extracting the spin Hamiltonian parameters required for the determination of structural information (*2–8*). Computer simulation of randomly orientated EPR spectra is performed in frequency space through the integration (*3, 9*)

$$S(B,\nu_c) = \sum_{i=0}^{M}\sum_{j=i+1}^{M} C\int_{\pi=0}^{\pi}\int_{\pi=0}^{\pi} \times |\mu_{ij}|^2 f[\nu_c - \nu_0(B), \sigma_\nu]d\cos\theta\, d\varphi, \quad [3]$$

where $S(B, \nu_c)$ denotes the spectral intensity, $|\mu_{ij}|^2$ is the transition probability, ν_c the microwave frequency, $\nu_0(B)$ the resonant frequency, σ_ν the spectral linewidth, $f[\nu_c - \nu_0(B), \sigma_\nu]$ a spectral lineshape function which normally takes the form of either Gaussian or Lorentzian, and C a constant which incorporates various experimental parameters. The summation is performed over all the transitions (i, j) contributing to the spectrum and the integration is performed over half of the unit sphere (for ions possessing triclinic symmetry), a consequence of time reversal symmetry (*1, 3*). For paramagnetic centres

[1] To whom correspondence should be addressed.

1090-7807/98 $25.00

with symmetries higher than triclinic only one or two octants are required.

Unlike most other spectroscopic techniques (nuclear magnetic resonance, infrared, and electronic absorption spectroscopy) which are frequency swept, EPR is a field-swept technique. In other words, the resonance condition $[h\nu_c = E_i(B_{\text{res}}) - E_j(B_{\text{res}})$; where E_i and E_j are the energies (eigenvalues) of the two spin states (eigenvectors) involved in the transition] is achieved by sweeping the magnetic field (varying B_{res} and hence E_i and E_j).

The methods used for determining B_{res} in the computer simulation of randomly oriented EPR spectra can be broadly classified into two categories, namely perturbation and matrix diagonalization methods.

In perturbation methods the energies of the spin states as a function of the field strength B are obtained from analytical expressions. This approach is computationally inexpensive but is limited largely to systems in which a dominant interaction exists and all the other interactions can be treated approximately as perturbations. This approach has been predominantly used to extract spin Hamiltonian parameters from EPR spectra of isolated paramagnetic centres which contain a single unpaired electron ($S = \frac{1}{2}$) (*2, 3, 10–16*) and exchange or dipole–dipole coupled binuclear centres ($S_{A_1} = S_{A_2} = \frac{1}{2}$) (*2–5*).

The second category involves matrix diagonalization and must be employed for calculating the eigenvalues and eigenvectors when perturbation theory breaks down (i.e., when two or more interactions have comparable energies). While the eigenvalues are used to calculate B_{res}, the eigenvectors are used to calculate the transition probability $|\mu_{ij}|^2$ (*3*).

In theory, this approach is general and can be applied to any spin system of choice. However, the numerical integration given in Eq. [3] can be very time-consuming as the process of searching for B_{res} for a given transition involves substantial computation and this searching process has to be repeated for every transition and for every orientation of the magnetic field. This often involves a very large number (100,000 or more) of matrix diagonalizations and memory requirements can be substantial if the spin space becomes large. Currently the most efficient algorithms for Hermitian matrix diagonalization are cubic processes $O(N^3)$ (where N is the order of the matrix) (*17*). As a consequence computer simulation programs employing this approach are performed in field space with symmetric lineshapes with a constant transition probability across a given resonance. Examples of computer simulation software which use this approach to simulate spectra from isolated paramagnetic centres include QPOW (*18*), EPR.FOR (*19*), MAGRES (*20, 21*), and MSPEN/MSGRA (*22*).

The "Sophe" method recently developed by Wang and Hanson features matrix diagonalization, a segmentation method employing second order eigenfield perturbation theory allowing B_{res} to be determined quickly, a new scheme for partitioning the unit sphere and the extremely efficient global cubic spline and local linear interpolation schemes for reducing the number of θ and ϕ orientations (*23–25*). While a 26-fold reduction in computational time can be achieved in the simulation of an orthorhombic Cr(III) EPR spectrum with Sophe, even larger reductions can be obtained with larger spin systems. The Sophe computer simulation software package allows the simulation of randomly orientated powder spectra described by either Eq. [1] or Eqs. [1] and [2] for all spin systems (i.e., $S_A \geq \frac{1}{2}$ or $S_{A_i} \geq \frac{1}{2}$, $S_{A_j} \geq \frac{1}{2}$: $i, j = 1, \ldots, N$; $j \neq i$) (*23–25*) and can easily be extended to other types of randomly orientated powder spectra in magnetic resonance.

In the Sophe method (*23, 24*), the B_{res} are calculated by matrix diagonalization only at a number of selected orientations which constitute the vertices of a given Sophe grid, (typically 190 orientations/vertices for orthorhombic symmetry). For all other orientations (normally in the thousands), B_{res} and $|\mu_{ij}|^2$ are obtained through the Sophe interpolation scheme. Such an approach has been demonstrated to be highly successful for simulating complicated EPR spectra (*26–28*).

However, all computer simulation programs, including Sophe, that employ matrix diagonalization, are not capable of performing the following functions satisfactorily:

(a) Tracing a given transition as a function of orientation in the presence of energy level crossings and anti-crossings (*29*).

(b) Tracing of surfaces (B_{res} as a function of orientation) which contain looping transitions (*29*). Looping transitions are transitions that fold back on themselves in orientational space.

(c) Performing the simulations in frequency space (*9*).

(d) Calculation of the transition probability across a resonance.

Thus, although the complete matrix diagonalization approach is far superior for general systems than perturbation methods, both methods are incapable of tracing the eigenpairs from one field position to another nearby position when there are holes in a transition surface, anti-level crossings, or looping transitions. Herein we describe the application and implementation of homotopy to the computer simulation of magnetic resonance spectra which allows the difficulties described above to be overcome.

HOMOTOPY

In other fields, the "homotopy" method, also known as the continuation or embedding method, has been shown to be efficient and useful for tracing eigenvalues and eigenvectors of a known diagonalization to an unknown diagonalization (*30, 31*). It has also been used to compute the complete eigendecomposition of symmetric tridiagonal matrices (*30, 31*). Homotopy works by constructing a function which connects

through smooth curves the eigenvalues and eigenvectors of one matrix to another. A similar method based on nonlinear least squares was used by Misra and Vasilopoulos (*32*) to trace the eigenvalues and hence the resonant field positions in single crystal EPR spectra.

The homotopy method can be used to trace the eigenvalues and eigenvectors (termed an eigenpair) for a given spin system as a function of orientation and magnetic field. Consequently, given a fixed microwave quantum ($h\nu_c$), transitions between a pair of eigenvectors can also be traced as a function of orientation and magnetic field, producing a complete eigensurface of eigenvalues and associated eigenvectors. This enables homotopy to uniquely follow the transition surface in the vicinity of anti-level crossings and looping transitions. Since the eigenvalues and eigenvectors are known as a function of orientation and magnetic field, the simulation of magnetic resonance spectra and in particular continuous wave EPR spectra can be correctly performed in frequency space.

The initial step in homotopy is the construction of a spin Hamiltonian matrix (H) based on an appropriate spin Hamiltonian (Eq. [1] or Eqs. [1] and [2]). This results in a matrix function in three variables, the Euler angles θ and ϕ, which reflect the angular dependence of the transitions, and the magnetic field **B.** For ease in further calculations this Hamiltonian matrix is split into field independent H_{indep} and field dependent H_{dep} (θ, ϕ, B) components. The eigenvalues (E) and eigenvectors (ψ) at an initial orientation, for example, $\theta = \phi = 0°$, are calculated from these matrices by solving the eigenvalue problem ($\mathcal{H}\psi = E\psi$).

The second step is to use an appropriate search algorithm to locate the resonant field positions B_{res} using the resonance condition

$$F = \Delta E = h\nu_c = E_i(\theta_1, \phi_1, B_{\text{res}}) - E_j(\theta_1, \phi_1, B_{\text{res}}) \qquad [4]$$

for an initial fixed set of Euler angles and a constant microwave quantum. The result of this search algorithm is two eigenpairs, corresponding to each transition, and a resonant field strength B_{res}. An example of such a search algorithm is described below. The probability of observing a transition between this pair of eigenvectors can be calculated by applying a mathematical formula to the eigenvectors.

The third step is to keep the magnetic field strength constant and calculate the resonant energy difference between the eigenvalues based strictly on changes to the Euler angles. In particular, the energy levels are traced from one fixed position (θ_0, ϕ_0) to another fixed position (θ_1, ϕ_1) which involves a change in one or both of the Euler angles. From the theory developed for the homotopy method we know that for an energy level $E(\theta_0, \phi_0, B_0)$ with a corresponding eigenvector $\psi_1(\theta_0, \phi_0, B_0)$ (*31*), the derivative of the eigenvalue E_i with respect to the homotopy variable T is given by

$$E_i'(\theta_0, \phi_0, B_0) = \psi_i(\theta_0, \phi_0, B_0)^T(H(\theta_0, \phi_0, B_0) - H(\theta_1, \phi_1, B_1))\psi_i(\theta_0, \phi_0, B_0). \qquad [5]$$

This equation is equivalent to the Rayleigh quotient (*33*) of the difference of the field dependent Hamiltonian at the two points. By using this formula and varying only θ and ϕ we can find an approximate spatial derivative of the eigenvalue, and thus the change in spin state due to spatial variations. Having found the derivatives for the two eigenvalues of interest, we can then estimate the eigenvalues at the new orientation (θ_1, ϕ_1). With these estimates of the new eigenvalues we can find the eigenvectors by solving the equation

$$(H(\theta_1, \phi_1, B_0) - E_i(\theta_1, \phi_1, B_0))\psi_i(\theta_1, \phi_1, B_0) = 0. \qquad [6]$$

We can then get a better estimate of each eigenvalue from the Rayleigh quotient (*33*) of the new eigenvector,

$$E(\theta_1, \phi_1, B_0) = \psi_i(\theta_1, \phi_1, B_0)^T H(\theta_1, \phi_1, B_0)\psi_i(\theta_1, \phi_1, B_0) \qquad [7]$$

and then calculate a new eigenvector corresponding to this new eigenvalue. Thus we iterate between estimates of the eigenvalue and the eigenvector until convergence (defined by the tolerance parameter $\delta_1 = 1.0 \times 10^4 \times \text{epsilon} \times |E|$), or the maximum number of iterations (n_1, typically 5) is exceeded. Epsilon is defined as the smallest difference between two double precision numbers and for a Silicon Graphics R5000 O2 workstation with 32 bit libraries equals 2.220446×10^{-16}. If the maximum number of iterations is exceeded for either eigenvalue, the total spatial distance is halved, and this step is repeated.

After having independently traced the two eigenpairs of interest from one spatial location (θ, ϕ) to another, the next step, step four, is to find the resonant field positions at the new orientation. This is accomplished by using another variation of the Homotopy algorithm. From Eqs. [4] and [5] where B is varied and θ and ϕ are held constant, we can find the derivative of the function F at (θ_1, ϕ_1, B_0)

$$F_B' = E_i'(\theta_1, \phi_1, B_0) - E_j'(\theta_1, \phi_1, B_0). \qquad [8]$$

We can now update the correction to the resonant field position B_{res},

$$\Delta B = -F/F_B'$$
$$B_1 = B_0 + \Delta B. \qquad [9]$$

Using this new value for B we can update the energies, E_i and E_j with the Rayleigh Quotient method and check the resonance condition (Eq. [4]). If the condition is not satisfied, we continue

to take new steps ΔB until Eq. [4] is satisfied, or until the maximum number of steps (n_2, typically 7) is exceeded. Upon convergence we return to step three and take a new spatial step. In general, this step ΔB is confined to be within some tolerance range ($\delta_2 = 1.0 \times 10^6 \times \text{epsilon} = 2.220446 \times 10^{-6}$), if this is not achieved, or if too many steps are required, then the algorithm goes back to step three halving the total spatial distance. This method will allow the calculation of the transition probability (from the eigenvectors) across a given transition line and in turn enables simulations to be performed in frequency space.

The implementation of homotopy to the analysis of randomly orientated EPR spectra is described below.

Set up Hamiltonian matrix defined by Eqs. [1] and [2] (Step 1)
  calculate the eigenvectors and eigenvalues at θ_0,ϕ_0 *by solving* $\mathcal{H}\psi = E\psi$
Locate resonant field positions B_{res} *(Step 2)*
Trace Eigenpath from θ_0,ϕ_0 *to* θ_1,ϕ_1 *(Step 3)*
  Set the tolerance δ_1*, the maximum iteration number,* n_1*,* $\Delta\theta$*, and* $\Delta\phi$
  $\theta = \theta_0 + \Delta\theta$
  $\phi = \phi_0 + \Delta\phi$
  Do
    Use $E(\theta_0,\phi_0,B_0)$ *and* $E'(\theta_0,\phi_0,B_0)$ *to predict* $E(\theta,\phi,B_0)$ *for the eigenvectors* ψ_i *and* ψ_j*.*
    Call Rayleigh Quotient Iteration (H, $E_i(\theta, \phi, B_0)$*,* $\psi_i(\theta, \phi, B_0)$*,* n_1*,* δ_1*)*
    Call Rayleigh Quotient Iteration (H, $E_j(\theta, \phi, B_0)$*,* $\psi_j(\theta, \phi, B_0)$*,* n_1*,* δ_1*)*
    If Rayleigh Quotient Iteration converged
      $\theta_1 = \theta$
      $\phi_1 = \phi$
      Exit
    Else
      $\Delta\theta = \Delta\theta/2$
      $\theta = \theta_0 + \Delta\theta$
      $\Delta\phi = \Delta\phi/2$
      $\phi = \phi_0 + \Delta\phi$
    End if
  While Rayleigh Quotient has not converged
End
Find the resonant field position B_{res} *(Step 4)*
  Set the tolerance δ_2 *and the maximum iteration number,* n_2*.*
  $B = B_0$
  Do i
    $F_B = E_i(\theta_1, \phi_1, B) - E_j(\theta_1, \phi_1, B)$
    $F'_B = E'_i(\theta_1, \phi_1, B) - E'_j(\theta_1, \phi_1, B)$
    $\Delta B = -F_B/F'_B$
    $B = B + \Delta B$
    Call Rayleigh Quotient Iteration (H, $E_i(\theta_1, \phi_1, B)\psi_i(\theta_1, \phi_1, B)$*,* n_2*,* δ_2*)*
    Call Rayleigh Quotient iteration (H, $E_j(\theta_1, \phi_1, B)\psi_j(\theta_1, \phi_1, B)$*,* n_2*,* δ_2*)*
    If Rayleigh Quotient Iteration converged and $\delta_2 < n_2$
      If $F_B - h\nu_c < \delta_2$
        $B_{res} = B$
        Exit
      End if
    Else
      $\Delta\theta = \Delta\theta/2$
      $\theta = \theta_0 + \Delta\theta$
      $\Delta\phi = \Delta\phi/2$
      $\phi = \phi_0 + \Delta\phi$
      Go to Step 3
    End if
    End do
End

The Rayleigh quotient iteration method (*33*) is used to determine both the eigenvalue and the eigenvector of a symmetric matrix.

Rayleigh Quotient Iteration(H, E, ψ*, n,* δ*)*
  $\psi_0 = \psi/\|\psi\|$
  $\mu_0 = E$
  For $i = 0, \ldots, n - 1$
    $y_i = (H - \mu_i I)^{-1}\psi_i$
    $\psi_{i+1} = y_i/\|y_i\|$
    $\mu_{i+1} = \psi_{i+1}^T H\psi_{i+1}$
    If $(\|\mu_{i+1} - \mu_i\| < \delta)$ *then*
      $\lambda = \mu_{i+1}$
      $\psi = \psi_{i+1}$
      Return success
    Endif
  End for loop

TABLE 1
Complexity Analyses for Matrix Diagonalization and Homotopy

Matrix diagonalization	
Procedure	Computation time
Tri-diagonalize H matrix.	$2/3\ N^3$
Diagonalize H matrix with an iterative QR method.[a]	8–10 N^3
Repeat diagonalization 200 times for each orientation (θ, ϕ).	$\sim$2000 N^3
Total computation time for $m^2/2$ orientations.	$\sim$2000 $N^3\ m^2/2$
Homotopy	
Tri-diagonalize H matrix.	$2/3\ N^3$
Rayleigh Quotient Iteration.[b]	15–20 N
Find Ψ from the original H matrix.	$2\ N^2$
Repeat $\sim$4 times to trace transition surface from one orientation to another.	$\sim 8/3\ N^3$
This calculation is repeated for d allowed transitions.	$\sim 8/3\ d\ N^3$
Total computation time for $m^2/2$ angular orientations.	$\sim 8/3\ d\ N^3\ m^2/2$

[a] Determine all E, Ψ of tri-diagonal H matrix.
[b] Using the tri-diagonal H matrix.

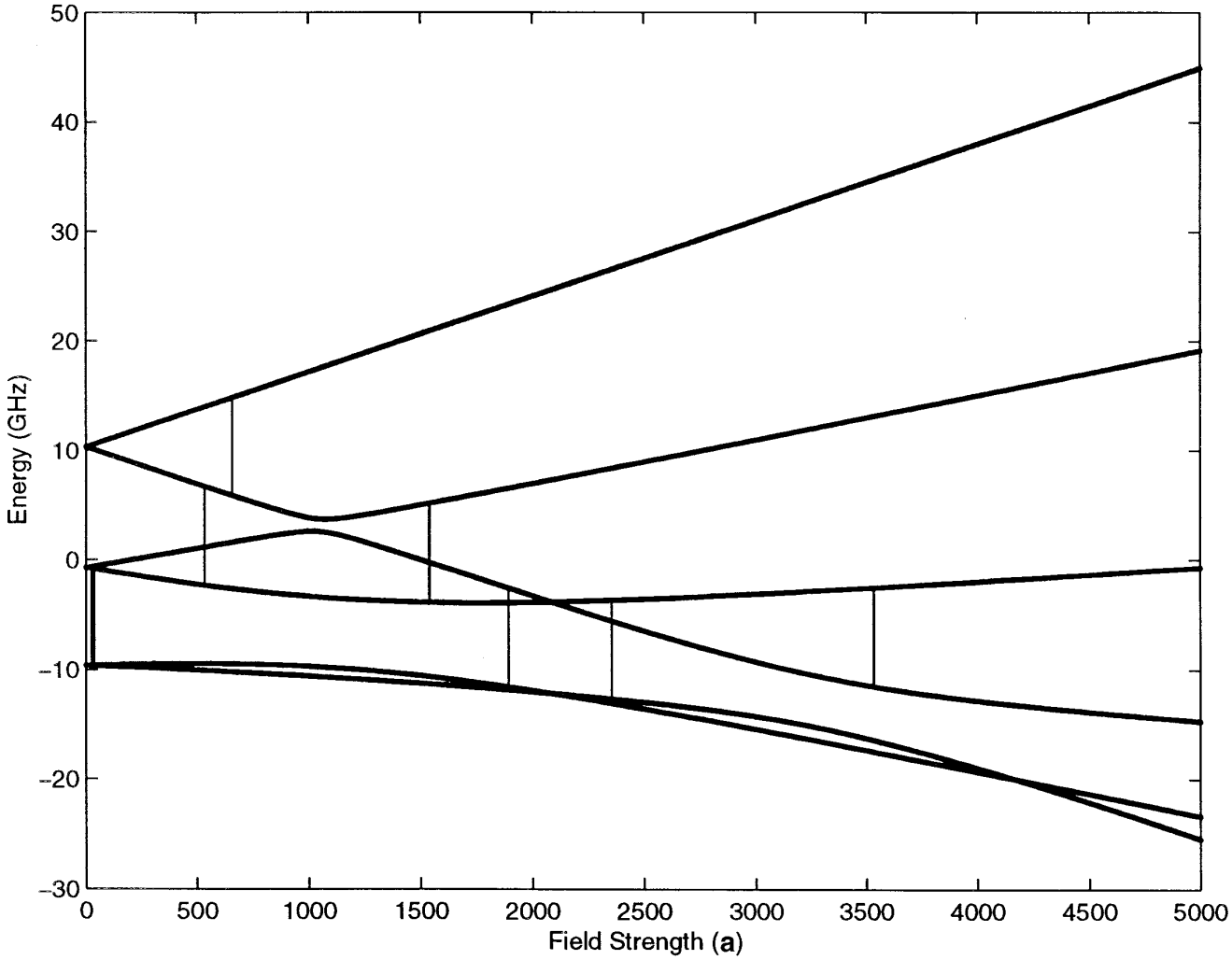

FIG. 1. An energy level diagram for a high-spin Fe(III) complex ($D = 0.1$ cm^{-1}, $E/D = 0.25$, $g = 2.0$, $\nu = 9.0$ GHz) at $\theta = 0°$ and $\phi = 0°$. Energy level numbers one through six correspond to levels in increasing energy.

Return failure
End

Application of homotopy to a continuously varying transition surface (for example, Fig. 2) is fairly straight forward. Given a single point on the surface, a method could just produce a line of eigenpair points along the θ axis, and then from every point on the line sweep out along the ϕ axis. However, such an algorithm will not find the complete surface if looping transitions are present (Fig. 3). Using this fundamental method, there are three possible cases when the surface will not be completed. The first two cases involve the comparison between two adjacent lines (i.e., two lines along the ϕ axis). If one line turns and the other doesn't, or if there is a great difference in B values between adjacent points, then part of the surface could be missing, for example, Fig. 4b. The third case is a surface that has a fairly complicated boundary and does not exist for the entire spatial dimension field.

The following modifications to homotopy described herein provide a solution to these problems. In step three, homotopy attempts to trace the eigenvalues from one angular position to another. If homotopy is unsuccessful, then the spatial distance is halved and the step is repeated. If the spatial distance falls below a certain level, then there are two possibilities—either the edge of the surface has been reached or a turn has been found. To investigate the possibility of a turn, homotopy is used to trace the eigenvalues in the reverse spatial direction. There is then the problem of whether a turn is being followed, or whether the previously found eigenpairs are being rediscovered. To ensure that a turn is indeed being followed the adjustments of B are checked. In general when B is adjusted, ΔB is confined to be within plus or minus a given tolerance, otherwise an error is produced. In the vicinity of a possible turn, ΔB is restricted further. If B was increasing prior to the possible turn, then B is confined to increase after the turn. If B was decreasing before the

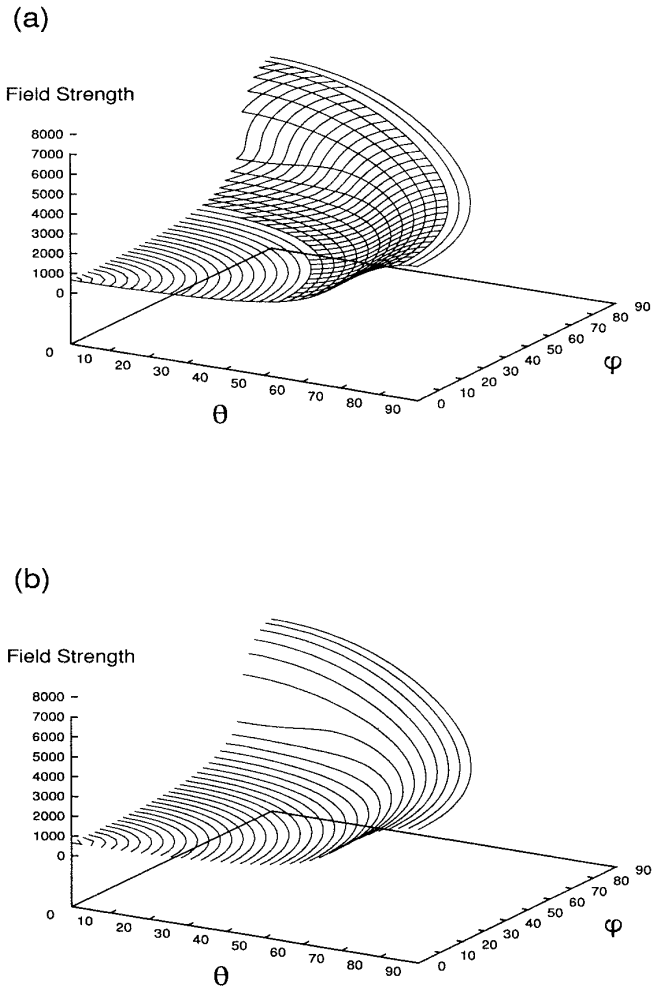

FIG. 2. Transition surface between levels 5 and 6 as a function of θ, ϕ, and B for a high-spin Fe(III) complex ($D = 0.1$ cm^{-1}, $E/D = 0.25$, $g = 2.0$, $\nu = 9.0$ GHz). Calculated using (a) homotopy and (b) matrix diagonalization, Sophe.

turn, then it will decrease after the turn. If homotopy continues to find eigenvalues with these restrictions imposed then a turn occurred, otherwise the edge of the surface was found.

A comparison of the complexity analyses for matrix diagonalization ($\sim 1000\, N^3\, m^2$) and homotopy ($\sim 4/3\, d\, N^3\, m^2$), Table 1, reveals that providing the number of transitions (d) is less than 75, homotopy will be computationally more efficient than matrix diagonalization.

APPLICATION OF HOMOTOPY TO AN $S = \frac{5}{2}$ SPIN SYSTEM

Homotopy has been tested for a high-spin Fe(III) system $S = \frac{5}{2}$ ($D = 0.1$ cm^{-1}, $E/D = 0.25$, $g = 2.0$) for which the second order fine structure spin Hamiltonian is

$$\mathcal{H} = g\beta \mathbf{B} \cdot \mathbf{S} + D\left[S_z^2 - \frac{1}{3}S(S+1)\right] + E(S_x^2 - S_y^2). \quad [10]$$

With the microwave quantum ($\nu = 9.0$ GHz) set to be slightly smaller than the zero-field splittings, multiple transitions can occur between a given pair of energy levels (Fig. 1). For example, between levels 2 and 4 (numbered in increasing energy), three transitions at $B_{res} = 35.25$, 1892.0, and 2355.0 mT are detected.

The power of homotopy in comparison to matrix diagonalization is clearly demonstrated in Figs. 2, 3, and 4 which compare transition surfaces from the two methods for particular transitions arising from an $S = \frac{5}{2}$ spin system. Figure 2 shows the transition surfaces between levels 5 and 6. The homotopy surface (Fig. 2a) shows exactly the same structure as calculated by matrix diagonalization (Fig. 2b). This transition surface varies continuously as a function of the Euler angles and the magnetic field B.

Table 2 gives the results of comparisons between homotopy and the matrix diagonalization, where the following information is given in the columns:

(1) the transition levels,

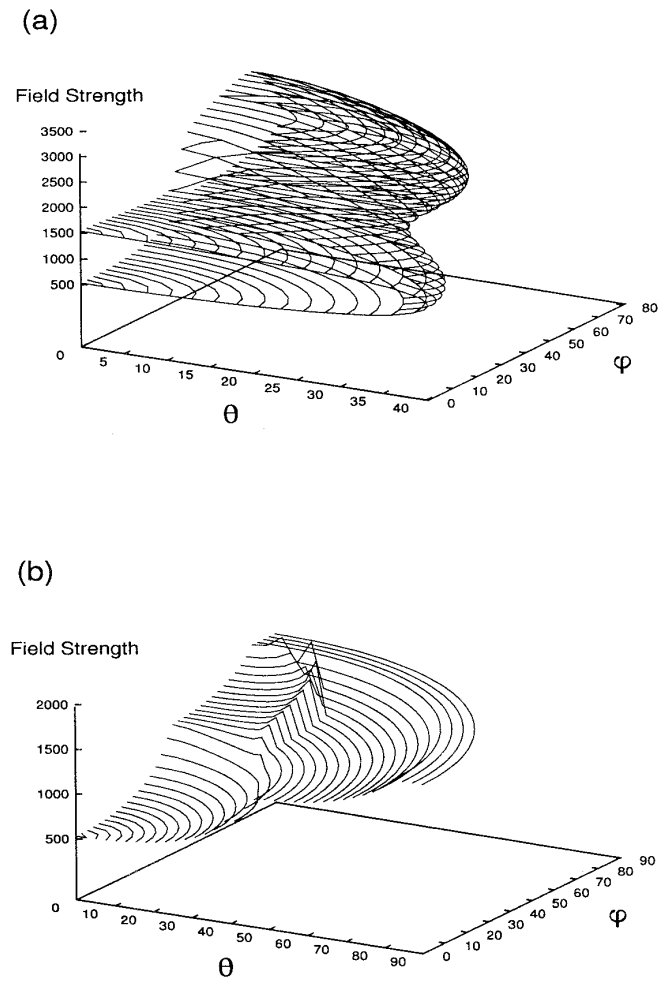

FIG. 3. Transition surface between levels 3 and 5 as a function of θ, ϕ, and B for a high-spin Fe(III) complex ($D = 0.1$ cm^{-1}, $E/D = 0.25$, $g = 2.0$, $\nu = 9.0$ GHz). Calculated using (a) homotopy and (b) matrix diagonalization, Sohpe.

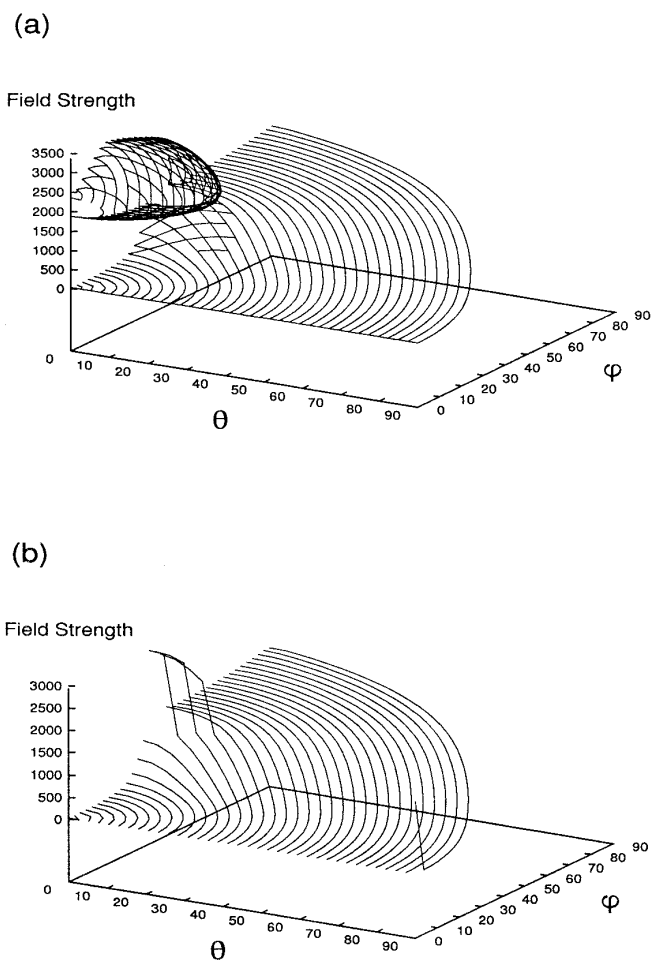

FIG. 4. Transition surface between levels 2 and 4 as a function of θ, ϕ, B for a high-spin Fe(III) complex ($D = 0.1$ cm^{-1}, $E/D = 0.25$, $g = 2.0$, $\nu = 9.0$ GHz). Calculated using (a) homotopy and (b) matrix diagonalization, Sophe.

(2) the relative difference (RA) between the Sophe points calculated using the two methods,

$$RA = 1/n^* \frac{\sum |B_{Matrix\ Diagonalization} - B_{Homotopy}|}{B_{Homotopy}}, \qquad [11]$$

(3) the total number of Sophe points computed,

(4) the number of erroneous data points where the magnetic field value for matrix diagonalization and homotopy do not agree, or where matrix diagonalization found an erroneous B value, and

(5) the number of multiple-valued Sophe points calculated by homotopy for which the matrix diagonalization routine may have calculated multiple points but Sophe was unable to complete the surface. Consequently only the lowest valued point has been reported.

Clearly, homotopy reproduces the surface obtained by matrix diagonalization between levels 5 and 6 as the relative error between the two methods is very small 4.104334×10^{-5}. The transition surface from level 3 to level 5 shown in Fig. 3 is an example of a looping transition in which the transition surface folds back on itself. While the surface is fully defined by homotopy (Fig. 3a), the surface calculated by matrix diagonalization is incomplete and erroneous since there are no transitions between levels 3 and 5 when $\theta > 40°$ (Fig. 3b). In Fig. 4 an anti-level crossing between levels 2 and 4 is graphed. Homotopy (Fig. 4a) resolves the complete structure while matrix diagonalization completes only the mostly continuous lower transition (Fig. 4b). In this case matrix diagonalization may have found multiple points. Matrix diagonalization may have discarded some points in completing the surface, as it is unable to make a connection between the multivalued points. Note that the unmatched homotopy points indicate structure not revealed with matrix diagonalization, while the points where matrix diagonalization and homotopy do not agree indicate erroneous points calculated by matrix diagonalization.

Randomly orientated spectra calculated with homotopy and matrix diagonalization are shown in Figs. 5a and 5b, respectively. Clearly there is excellent agreement between the two methods for this spin system. For the high-spin Fe(III) system described above with $N = 100$ (the number of θ orientations in the Sophe grid) and 100 field intervals for matrix diagonalization, matrix diagonalization took 535.661 s while homotopy took 149.126 s on a Silicon Graphics R5000 O2 workstation with 256 Mb of memory. For other spin systems that we have examined, homotopy is at least twice as fast as matrix diagonalization.

CONCLUDING REMARKS

Homotopy has been implemented within the XSophe/Sophe electron paramagnetic resonance computer simulation suite, wherein it is used to find the eigenvalues and associated eigenvectors of the special class of matrices generated in the computer simulation of magnetic resonance spectra. In particular, by directly tracing the eigenfunctions in parameter space it can:

TABLE 2
Comparison of Homotopy and Matrix Diagonalization Methods

Levels	Relative accuracy (RA)	Total Sophe points (n)	Erroneous data points[a]	Unmatched homotopy points[b]
2 4	1.071440×10^{-3}	666	2	156
3 5	1.025706×10^{-4}	666	411	255
5 6	4.104334×10^{-5}	666	0	0

[a] The number of erroneous data points where the magnetic field value for matrix diagonalization and homotopy do not agree, or where matrix diagonalization found an erroneous B value.

[b] The number of multiple valued Sophe points calculated by homotopy for which matrix diagonalization did not return a multiple valued point.

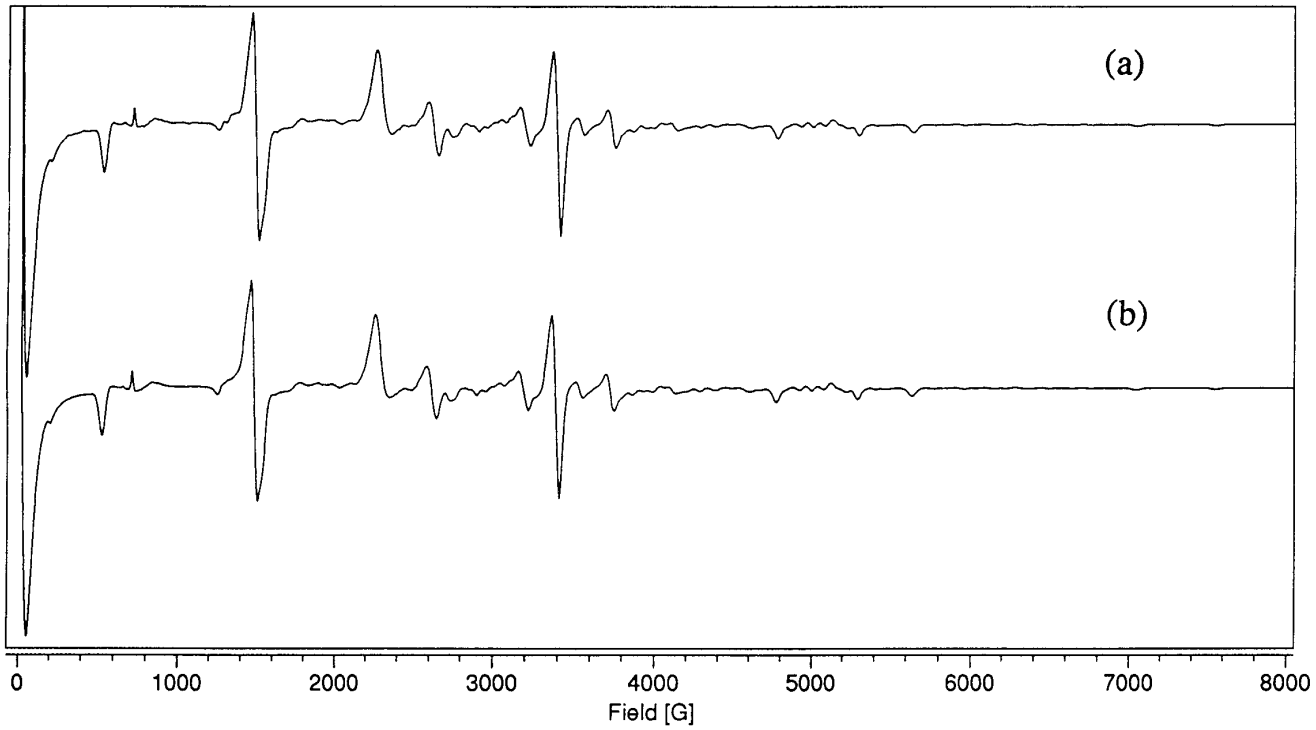

FIG. 5. Randomly orientated spectra for a high-spin Fe(III) complex with $D = 0.1$ cm^{-1}, $E/D = 0.25$, $g = 2.0$, and $\nu = 9.0$ GHz. Calculated with (a) homotopy and (b) matrix diagonalization.

—trace a given transition as a function of orientation ($\theta = 0 \rightarrow 180°$, $\phi = 0 \rightarrow 180°$) in the presence of energy level anti-crossing,
—trace looping transitions, and
—perform the simulations in frequency space.

Since this method is also theoretically less expensive than matrix diagonalization, when combined with the Sophe interpolation scheme it should result in significant reductions in computational time for the simulation of EPR spectra without sacrificing accuracy. Homotopy may also be used in conjunction with other partition schemes, for example, the "Apple-peel" (*3*), "Igloo" (*18*), "Spiral" (*19*), and "Triangular" (*34*) methods and perturbation theory.

Consequently, in conjunction with the Sophe partition scheme homotopy improves the quality of simulated spectra, allows the analysis of more complicated EPR spectra from complex spin systems, and reduces the computational time compared with matrix diagonalization. The method can also be extended to the simulation of field dependent CW-ENDOR, ESEEM, pulsed ENDOR, solid state NMR, and nuclear quadrupole resonance spectra.

ACKNOWLEDGMENTS

The authors thank Professor Sushil Misra for helpful discussions and the Australian Research Council for financial support.

REFERENCES

1. A. Abragam and B. Bleaney, "Electron Paramagnetic Resonance of Transition Ions," Clarendon, Oxford (1970).
2. F. E. Mabbs and D. C. Collison, "Electron Paramagnetic Resonance of Transition Metal Compounds," Elsevier, Amsterdam (1992).
3. J. R. Pilbrow, "Transition Ion Electron Paramagnetic Resonance," Clarendon, Oxford (1990).
4. A. Bencini and D. Gatteschi, "EPR of Exchange Coupled Systems," Springer-Verlag, Berlin (1990).
5. T. D. Smith and J. R. Pilbrow, *Coord. Chem. Rev.* **13,** 173 (1974).
6. (*a*) J. D. Swalen and H. M. Gladney, *IBM J. Res. Dev.* **8,** 515 (1964); (*b*) J. D. Swalen, T. R. L. Lusebrink, and D. Ziessow, *Magn. Reson. Rev.* **2,** 165 (1973).
7. P. C. Taylor, J. F. Baugher, and H. M. Kriz, *Chem. Rev.* **75,** 203 (1975).
8. H. L. Vancamp and A. H. Heiss, *Magn. Reson. Rev.* **7,** 1 (1981).
9. J. R. Pilbrow, *J. Magn. Reson.* **58,** 186 (1984).
10. G. R. Sinclair, "Modelling Strain Broadened EPR Spectra," Ph.D. thesis, Monash University (1988).
11. A. L. Van den Brenk, D. P. Fairlie, G. R. Hanson, L. R. Gahan, C. J. Hawkins, and A. Jones, *Inorg. Chem.* **33,** 2280 (1994).
12. (*a*) D. J. Lowe, *Biochem. J.* **171,** 649 (1978); (*b*) G. D. Markham, B. D. Nageswara Rao, and G. H. Reed, *J. Magn. Reson.* **33,** 595 (1979).
13. P. C. Taylor and P. J. Bray, *J. Magn. Reson.* **2,** 305 (1970).
14. P. H. Reiger, *J. Magn. Reson.* **50,** 485 (1982).
15. J. C. Schwatrz, B. M. Hoffman, R. J. Krijek, and D. K. Atmatzidis, *J. Magn. Reson.* **36,** 259 (1979).

16. M. I. Scullane, L. K. White, and N. D. Chasteen, *J. Magn. Reson.* **47,** 383 (1982).

17. E. Anderson, Z. Bai, C. Bischof, J. Demmel, J. Dongarra, J. Du Croz, A. Greenbaum, S. Hammarling, A. McKenney, S. Ostrouchov, and D. Sorensen, "LAPACK Users' Guide," Soc. for Industr. & Appl. Math., Philadelphia (1992).

18. (*a*) R. L. Belford and M. J. Nilges, *in* "EPR Symposium 21st Rocky Mountain Conference, Denver, CO, 1979;" (*b*) A. M. Maurice, Ph.D. thesis, University of Illinois, Urbana, IL (1980); (*c*) M. J. Nilges, "Electron Paramagnetic Resonance Studies of Low Symmetry Nickel(I) and Molybdenum(V) Complexes," Ph.D. thesis, University of Illinois, Urbana, IL (1979).

19. M. J. Mombourquette and J. A. Weil, *J. Magn. Reson.* **99,** 37 (1992).

20. C. P. Keijzers, E. J. Reijerse, P. Stam, M. F. Dumont, and M. C. M. Gribnau, *J. Chem. Soc. Faraday Trans. I* **83,** 3493 (1987).

21. M. C. M. Gribnau, J. L. C. van Tits, and E. J. Reijerse, *J. Magn. Reson.* **90,** 474 (1990).

22. A. Kreiter and J. Hüttermann, *J. Magn. Reson.* **93,** 12 (1991).

23. D. Wang and G. R. Hanson, *J. Magn. Reson. A* **117,** 1 (1995).

24. D. Wang and G. R. Hanson, *Appl. Magn. Reson.* **11,** 401 (1996).

25. D. Wang and G. R. Hanson, "Computer Simulation of Magnetic Resonance Spectra," International Patent Application No. PCT/AU96/00534, 1996.

26. V. Grillo, G. R. Hanson, D. Wang, T. W. Hambley, L. R. Gahan, K. S. Murray, B. Moubaraki, and C. J. Hawkins, *Inorg. Chem.* **35,** 3568 (1995).

27. L. R. Gahan, V. A. Grillo, T. W. Hambley, G. R. Hanson, C. J. Hawkins, E. M. Proudfoot, B. Moubaraki, K. S. Murray, and D. Wang, *Inorg. Chem.* **35,** 1039 (1996).

28. W. Adam, C. van Barneveld, S. E. Bottle, H. Engert, G. R. Hanson, H. M. Harrer, C. Heim, W. M. Nau, and D. Wang, *J. Amer. Chem. Soc.* **118,** 3974 (1996).

29. D. Wang and J. R. Pilbrow, *J. Magn. Reson.* **77,** 411 (1988).

30. T. Y. Li and N. H. Rhee, *Numer. Math.* **55,** 265 (1989).

31. M. Oettli, Technical Report 205, Department Informatik, ETH, Zürich (1993), and references therein.

32. S. K. Misra and P. Vasilopoulos, *J. Phys. C* **13** (1980).

33. G. H. Golub and C. F. Van Loan, "Matrix Computations," Johns Hopkins Press, Baltimore (1983).

34. D. W. Alderman, M. S. Solum, and D. M. Grant, *J. Chem. Phys.* **84,** 3717 (1986).